Three-mode entanglement via tunneling-induced interference in a coupled triple-semiconductor quantum-well structure

Xin-You Lü[1,3,*] and Jing Wu[2]

[1]*School of Physics, Ludong University, Yantai 264025, People's Republic of China*
[2]*Institute of Advanced Nanophotonics State Key Lab of Modern Optical Instrumentation, Zhejiang University, Hangzhou 310027,*
People's Republic of China
[3]*Wuhan National Laboratory for Optoelectronics, Huazhong University of Science and Technology, Wuhan 430074,*
People's Republic of China
(Received 25 April 2010; published 22 July 2010)

A simple scheme is proposed to achieve three-mode continuous-variable (CV) entanglement in a coupled triple-semiconductor quantum-well (TSQW) structure via tunneling-induced interference. In the present scheme, the TSQW structure is trapped into a triply resonant cavity, and the tunneling-induced interference effects considered here are the key to realizing entanglement. By numerically simulating the dynamics of the system, we show that the strength of tunneling-induced interference can effectively influence the period of entanglement, and the generation of entanglement does not depend intensively on the initial condition of the cavity field in our scheme. As a result, the present research provides an efficient approach to achieve three-mode CV entanglement in a semiconductor nanostructure, which may have an impact on the progress of solid-state quantum-information theory.

I. INTRODUCTION

Quantum entanglement has become the investigative focus in the quantum optics and quantum-information fields and attracts much interest due to its wide applications in quantum teleportation, quantum cryptography, quantum computation, etc. [1–10]. In particular, continuous-variable (CV) entanglement has received increasing attention from physicists [11–13] due to its unconditionality for the implementation of many quantum-information processes [14–16]. A large amount of research has been devoted to the measurement [17–20] and generation [21–25] of two-mode CV entanglement in recent years. For example, Duan *et al.* [17] proposed a criterion to determine the inseparability of the two-mode CV system. Subsequently, Xiong *et al.* [21] studied the generation of two-mode CV entanglement in a three-level atomic system based on the quantum coherence induced by an external classical field. Moreover, along with the progress on quantum-information networks with many nodes, multimode CV entanglement [26–38] has become an important topic of research due to its ability to address different nodes in a quantum network. For example, van Loock and Furusawa [26] proposed a sufficient condition for judging genuine multipartite CV entanglement. Based on this sufficient condition, Aoki *et al.* realized experimentally a tripartite CV entangled state by using beam splitters to combine three independent squeezed vacuum states [27]. However, the beam splitter transformation is linear, and it is therefore difficult to obtain entangled beams of different frequencies based on their scheme. Subsequently, Hu *et al.* [37] proposed a scheme for realizing three-mode CV entanglement with different frequencies for each mode in a coherent atomic system, where quantum coherence is induced by a strong classical field. More recently, we also have researched the generation of fully three-mode CV entanglement in the tripartite-correlated emission laser

(CEL) [38], which is an extension of the work in Ref. [21] for realizing two-mode CV entanglement. The preceding description shows that three-mode CV entanglement can be realized in an atomic system based on the quantum-coherence effects induced by a classical field. However, the atom is a gaseous medium, and there are some defects in the flexibility of device fabrication for a gaseous medium.

In contrast, it has been shown that the semiconductor quantum well (SQW) has properties similar to those of atomic vapors such as discrete energy levels and controllable quantum-coherence effects, which are generated either by an external driving field or by interference in tunneling to an electronic continuum (i.e., tunneling-induced interference). In recent years, the SQW has attracted much attention due to its many inherent advantages compared to the atomic system, such as large electric dipole moments, high nonlinear optical coefficients, and great flexibility in device design via the choice of materials and structure dimensions [39–45]. Based on the corresponding quantum-coherence effects, gain without inversion [46], coherent population trapping [47], and electromagnetically induced transparency [48,49] have been realized in the SQW system. Recently, Lee *et al.* [50] proposed a triple-semiconductor quantum-well (TSQW) model with one ground subband and three excited subbands that are coupled by tunneling to the same electronic continuum. They demonstrated that two-color lasing without population inversion can be realized in this system based on tunneling-induced interference effects. Subsequently, coherent population trapping, double tunneling-induced transparency, slow light, transient gain without population inversion [51], and optical bistability [52] were studied in this system. All the mentioned characteristics of the SQW medium offer a feasible platform for realization of many quantum-information processes (e.g., quantum entanglement) in a solid-state semiconductor medium, which is significant for the progress of quantum-information theory. To the best of our knowledge, no related theoretical or experimental work has been carried out
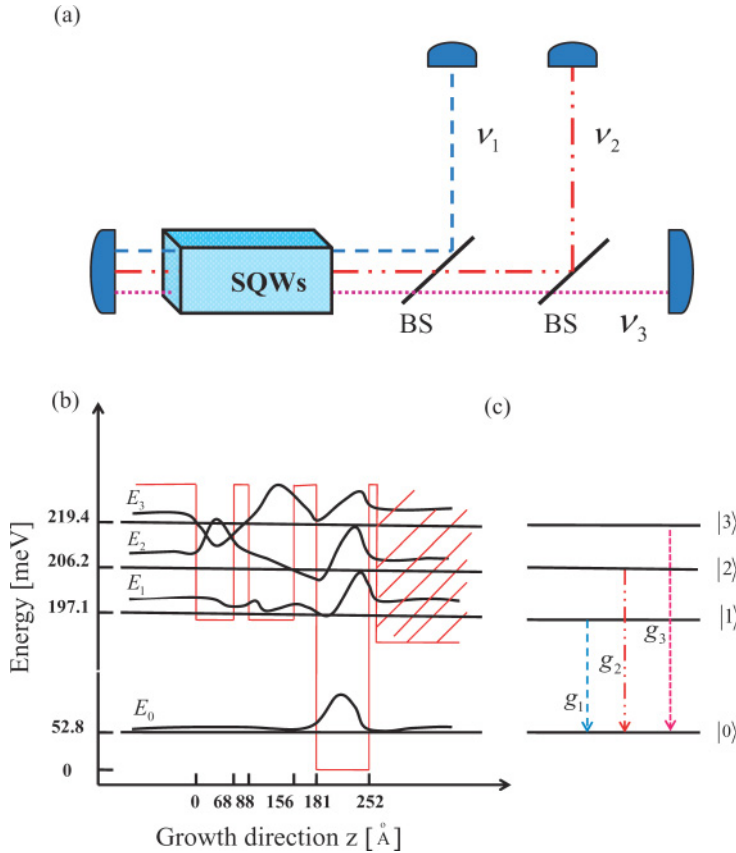
*xinyou_lv@163.com

FIG. 1. (Color online) (a) Possible arrangement of the experimental apparatus. The TSQW structure considered here is trapped into a triply resonant cavity. (b) Schematic band diagram of the TSQW structure consisting of a deep well and two shallow wells coupled by tunneling to a common continuum of energies through a thin barrier. The ground states of two shallow wells and the first excited state of the deep well mix to create three excited states of the system. The electronic wave functions of the ground state of the deep well and the three excited states are labeled $|0\rangle$, $|1\rangle$, $|2\rangle$, and $|3\rangle$. The TSQW structure is sandwiched by a pair of electrodes. (c) Schematic of the energy level arrangement under study. Three nondegenerate cavity modes, ν_1, ν_2, and ν_3, resonantly couple with the corresponding transition $|m\rangle \to |0\rangle$ ($m = 1, 2, 3$).

to realize three-mode CV entanglement in a TSQW system, which motivates the current work.

In this paper, based on the standard criteria proposed by van Loock and Furusawa [26], we propose a scheme for achieving fully three-mode CV entanglement in a TSQW medium, which is trapped in a nondegenerate triply resonant cavity (see Fig. 1). The root for the generation of entanglement in our scheme is the quantum-interference effects induced by tunneling between three excited states and the same electronic continuum (i.e., tunneling-induced interference). The major advantages of our scheme are as follows. (i) The TSQW medium studied here is a solid, which is much more practical than a gaseous medium (e.g., a cold atom) due to its flexible design and widely adjustable parameters. For example, the transition energies and dipole moments can be manipulated well by accurately tailoring their shapes and sizes, whereas they can hardly be found in the models for a cold atom medium [46]. (ii) In the present scheme, three-mode entanglement is generated based on tunneling-induced interference effects, which can be obtained without any additional classical field applied. From this viewpoint, it is simpler than the previous schemes, in which the required atomic coherence effect is induced by additional classical fields coupling the corresponding atomic transitions [37,38]. (iii) According to the corresponding experimental parameters in Ref. [50], the frequencies of intersubband transition in the TSQW are usually in the far- and midinfrared scopes. So the proposed system can serve as the source for generating infrared entangled lights (e.g., $\lambda_1 \simeq 8.6$ μm, $\lambda_2 \simeq 8.1$ μm, $\lambda_3 \simeq 7.5$ μm, corresponding to the present scheme), which may have wide applications in quantum communications.

The remainder of this paper is organized in four parts as follows. In Sec. II, we first describe the model under consideration and present the equation of motion for the reduced density operator of the cavity field ρ_f. In Sec. III, the generation of three-mode CV entanglement is demonstrated. Finally, we conclude with a brief summary in Sec. IV.

II. MODEL AND EQUATION

As shown in Fig. 1(a), we consider a three-mode CEL consisting of a TSQW medium inside a triply resonant cavity. The TSQW medium [see Fig. 1(b)] considered here is the same as that in Ref. [50] and it can be obtained by coupling two shallow 6.8-nm-thick $Al_{0.2}Ca_{0.8}As$ wells separated by a 2.0-nm-thick $Al_{0.4}Ca_{0.6}As$ barrier and a deep 7.1-nm-thick CaAs well to a common continuum ($Al_{0.165}Ca_{0.835}As$) through a 0.7-nm-thick $Al_{0.4}Ca_{0.6}As$ Al barrier. The deep well and its adjacent shallow well are separated by an $Al_{0.4}Ca_{0.6}As$ barrier 2.5 nm thick. In the present system, the ground states of the two shallow wells and the first excited state of the deep well mix to create three excited states of the system (labeled $|1\rangle$, $|2\rangle$, $|3\rangle$) due to the tunneling between different quantum wells. As shown in Fig. 1(c), the ground state of this system is labeled $|0\rangle$. Three nondegenerate cavity modes, ν_1, ν_2, and ν_3, resonantly couple with the transitions $|1\rangle \leftrightarrow |0\rangle$, $|2\rangle \leftrightarrow |0\rangle$, and $|3\rangle \leftrightarrow |0\rangle$, respectively. For convenience, we can choose the free Hamiltonian of this complex system $H_0 = \nu_1|1\rangle\langle 1| + \nu_2|2\rangle\langle 2| + \nu_3|3\rangle\langle 3| + \sum_{i=1-3} \nu_i a_i^\dagger a_i$. Then, under the dipole and rotating wave approximations, the interaction Hamiltonian of our system can be written in the interaction

picture as ($\hbar = 1$) [53–56]

$$H_I = [g_1 a_1 |1\rangle\langle 0| + g_2 a_2 |2\rangle\langle 0| + g_3 a_3 |3\rangle\langle 0| + \text{H.c.}], \quad (1)$$

where $a_i^\dagger$ and a_i ($i = 1\text{–}3$) are the creation and annihilation operators corresponding to three cavity modes. g_1, g_2, and g_3 are the corresponding electron-field coupling constants.

Using the density-matrix formalism, the reduced density equations of the field ρ_f can be obtained by taking a trace over the electron, which leads to

$$\dot{\rho}_f = -i \text{Tr}_e [H_I, \rho_{e\text{-}f}]$$
$$= (-ig_1[a_1^\dagger, \rho_{10}] - ig_2[a_2^\dagger, \rho_{20}] - ig_3[a_3^\dagger, \rho_{30}] + \text{H.c.}), \quad (2)$$

where $\rho_{e\text{-}f}$ is the full election-field density operator and $\rho_{10} = \langle 1|\rho_{e\text{-}f}|0\rangle$, $\rho_{20} = \langle 2|\rho_{e\text{-}f}|0\rangle$, and $\rho_{30} = \langle 3|\rho_{e\text{-}f}|0\rangle$. Then, according to the standard methods of laser theory [57], ρ_{10}, ρ_{20}, and ρ_{30} can be evaluated to first order in the coupling constants g_1, g_2, and g_3 as

$$\dot{\rho}_{30} = -\frac{\Gamma_{30}}{2}\rho_{30} + ig_3\rho_{33}^{(0)}a_3 + ig_2\rho_{32}^{(0)}a_2 + ig_1\rho_{31}^{(0)}a_1$$
$$- ig_3 a_3\rho_{00}^{(0)} - \frac{\kappa_{31}}{2}\rho_{10} - \frac{\kappa_{32}}{2}\rho_{20}, \quad (3a)$$

$$\dot{\rho}_{20} = -\frac{\Gamma_{20}}{2}\rho_{20} + ig_3\rho_{23}^{(0)}a_3 + ig_2\rho_{22}^{(0)}a_2 + ig_1\rho_{21}^{(0)}a_1$$
$$- ig_2 a_2\rho_{00}^{(0)} - \frac{\kappa_{21}}{2}\rho_{10} - \frac{\kappa_{32}}{2}\rho_{30}, \quad (3b)$$

$$\dot{\rho}_{10} = -\frac{\Gamma_{10}}{2}\rho_{10} + ig_3\rho_{13}^{(0)}a_3 + ig_2\rho_{12}^{(0)}a_2 + ig_1\rho_{11}^{(0)}a_1$$
$$- ig_1 a_1\rho_{00}^{(0)} - \frac{\kappa_{21}}{2}\rho_{20} - \frac{\kappa_{31}}{2}\rho_{30}, \quad (3c)$$

where $\rho_{mn}^{(0)}$ is the corresponding zeroth-order matrix element and $\rho_{00}^{(0)} = 1$. This assumption corresponds to a situation in which the electron is initially prepared in the ground state $|0\rangle$. It should be pointed out that we have added phenomenologically the corresponding population decay rates and dephasing decay rates in Eqs. (3). The population decay rates from subband $|m\rangle$ to $|0\rangle$, denoted γ_m ($m = 1,2,3$), are due primarily to longitudinal optical phonon emission events at low temperature. The total decay rates Γ_{m0} are given by $\Gamma_{10} = \gamma_1 + \gamma_{10}^{\text{dph}}$, $\Gamma_{20} = \gamma_2 + \gamma_{20}^{\text{dph}}$, and $\Gamma_{30} = \gamma_3 + \gamma_{30}^{\text{dph}}$, where γ_{m0}^{dph}, determined by electron-electron, interface roughness, and phonon scattering processes, is the dephasing decay rate of the quantum coherence of the $|m\rangle \leftrightarrow |0\rangle$ transition. κ_{mn} denotes the coupling between the excited states $|m\rangle$ and $|n\rangle$ and occurs due to tunneling-induced interference [50–52]. It gives rise to the coherent phenomena that appear in this system and describes the process in which a phonon is emitted by subband $|m\rangle$ and is recaptured by subband $|n\rangle$. This coherence is the key to realizing entanglement in our scheme, which replaces the atomic coherence induced by the additional classical field in the previous scheme [21,37,38]. The principle of generating tunneling-induced interference can be summarized briefly as follows. As shown in Fig. 1, levels $|1\rangle$, $|2\rangle$, and $|3\rangle$ are all superposition states of the ground states of the two shallow wells and the first excited state of the deep well. Then, because the deep well is strongly coupled to a continuum via a thin barrier, the decay from the first excited state of

the deep well to the continuum inevitably results in these three dependent decay pathways: from levels $|1\rangle$, $|2\rangle$, and $|3\rangle$ to the common continuum. So the three decay pathways are correlative, and they strongly affect each other, which results in tunneling-induced interference in this TSQW system.

Via solving Eqs. (3) and substituting the expressions ρ_{30}, ρ_{20}, and ρ_{10} into Eq. (2), we obtain the following master equation for the density operator of cavity ρ_f:

$$\dot{\rho}_f = [\alpha_{11}(a_1^\dagger a_1\rho_f - a_1\rho_f a_1^\dagger) + \alpha_{12}(a_1^\dagger a_2\rho_f - a_2\rho_f a_1^\dagger)$$
$$+ \alpha_{13}(a_1^\dagger a_3\rho_f - a_3\rho_f a_1^\dagger) + \alpha_{21}(a_2^\dagger a_1\rho_f - a_1\rho_f a_2^\dagger)$$
$$+ \alpha_{22}(a_2^\dagger a_2\rho_f - a_2\rho_f a_2^\dagger) + \alpha_{23}(a_2^\dagger a_3\rho_f - a_3\rho_f a_2^\dagger)$$
$$+ \alpha_{31}(a_3^\dagger a_1\rho_f - a_1\rho_f a_3^\dagger) + \alpha_{32}(a_3^\dagger a_2\rho_f - a_2\rho_f a_3^\dagger)$$
$$+ \alpha_{33}(a_3^\dagger a_3\rho_f - a_3\rho_f a_3^\dagger) + \text{H.c.}] - \kappa_1(a_1^\dagger a_1\rho_f - \rho_f a_1^\dagger a_1$$
$$- 2a_1\rho_f a_1^\dagger) - \kappa_2(a_2^\dagger a_2\rho_f - \rho_f a_2^\dagger a_2 - 2a_2\rho_f a_2^\dagger)$$
$$- \kappa_3(a_3^\dagger a_3\rho_f - \rho_f a_3^\dagger a_3 - 2a_3\rho_f a_3^\dagger), \quad (4)$$

where the coefficients α_{mn} ($m,n = 1,2,3$) are given by

$$\alpha_{11} = \frac{2g_1^2(\kappa_{32}^2 - \Gamma_{30}\Gamma_{20})}{D},$$
$$\alpha_{12} = \frac{2g_1 g_2(\kappa_{31}\kappa_{32} - \kappa_{21}\Gamma_{30})}{D},$$
$$\alpha_{13} = \frac{2g_1 g_3(\kappa_{21}\kappa_{32} - \kappa_{31}\Gamma_{20})}{D},$$
$$\alpha_{21} = \frac{2g_2 g_1(\kappa_{31}\kappa_{32} - \kappa_{21}\Gamma_{30})}{D},$$
$$\alpha_{22} = -\frac{2g_2^2(\kappa_{31}^2 - \Gamma_{10}\Gamma_{30})}{D}, \quad (5)$$
$$\alpha_{23} = \frac{2g_2 g_3(\kappa_{21}\kappa_{31} - \kappa_{32}\Gamma_{10})}{D},$$
$$\alpha_{31} = \frac{2g_3 g_1(\kappa_{21}\kappa_{32} - \kappa_{31}\Gamma_{20})}{D},$$
$$\alpha_{32} = \frac{2g_3 g_2(\kappa_{21}\kappa_{31} - \kappa_{32}\Gamma_{10})}{D},$$
$$\alpha_{33} = \frac{2g_3^2(-\kappa_{21}^2 + \Gamma_{10}\Gamma_{20})}{D},$$

with

$$D = -2\kappa_{21}\kappa_{31}\kappa_{32} + \kappa_{32}^2\Gamma_{10} + \kappa_{21}^2\Gamma_{30} + \Gamma_{20}(\kappa_{31}^2 - \Gamma_{10}\Gamma_{30}). \quad (6)$$

It should be pointed out that, in the preceding calculations, the dampings of the cavity modes have been added phenomenologically, and $\kappa_1, \kappa_2, \kappa_3$ denote the decay rates of the three cavity modes, respectively.

Before starting the next section, let us qualitatively explain the basis of fully generating three-mode CV entanglement based on our scheme. Here, the essential reason for generating three-mode CV entanglement is the tunneling-induced interference, which is similar to the coherence effect induced by the classical field in the atomic system. Specifically, per the preceding description, coupling between level $|1\rangle$ and level $|2\rangle$ (denoted κ_{21}) due to electron tunneling will induce the corresponding quantum-coherence effects and make the modes a_1 and a_2 entangled. Similarly, the coupling between level

$|i\rangle$ and level $|3\rangle$ (denoted κ_{3i}, with $i = 1,2$) will make modes a_i and a_3 entangled. Therefore, the three-mode cavity field considered here is not bipartite separable, that is, the bipartite decompositions $a_1|a_2a_3$, $a_2|a_1a_3$, and $a_3|a_1a_2$ are all entangled. In other words, the three-mode cavity field considered here is a fully three-mode CV entangled state in this situation.

III. THE GENERATION OF THREE-MODE CONTINUOUS-VARIABLE ENTANGLEMENT

In this section, we discuss the generation of fully three-mode CV entanglement based on the sufficient inseparability criteria for a three-mode CV system [26]. As shown in Refs. [58] and [59], a three-mode CV state is fully separable if and only if the density operator for the state ρ can be written as a convex combination of product state

$$\rho = \sum_j p_j \rho_j^{(1)} \otimes \rho_j^{(2)} \otimes \rho_j^{(3)}, \qquad (7)$$

with $p_j \geqslant 0$ and $\sum_j p_j = 1$. $\rho_j^{(1)}$, $\rho_j^{(2)}$, and $\rho_j^{(3)}$ are the normalized states of three field modes, respectively. A three-mode CV state is fully entangled if it is not bipartite separable. According to the criteria derived in Ref. [26], the three-mode cavity field considered here is fully entangled if any pair of the following inequalities is satisfied simultaneously:

$$V_{12} = V(X_1 - X_2) + V(Y_1 + Y_2 + Y_3) \leqslant 4, \qquad (8a)$$

$$V_{13} = V(X_1 - X_3) + V(Y_1 + Y_2 + Y_3) \leqslant 4, \qquad (8b)$$

$$V_{23} = V(X_2 - X_3) + V(Y_1 + Y_2 + Y_3) \leqslant 4, \qquad (8c)$$

where $X_m = a_m + a_m^\dagger$ and $Y_m = -i(a_m - a_m^\dagger)$ ($m = 1,2,3$) are the quadrature operators for the three cavity modes, and $V(A) = \langle A^2 \rangle - \langle A \rangle^2$ (A denotes an arbitrary operator).

Then, with the help of Eq. (4), we numerically simulate the dynamical evolution of this system for different values of parameters, as illustrated in Figs. 2–6. Note that, in the following numerical calculations, the choices of the parameters

are based on the investigation in Refs. [50] and [51]. It is shown in the figures that three-mode CV entanglement can be realized in the TSQW system based on tunneling-induced interference effects. In addition, the numerical results show that the entanglement period can be prolonged effectively via enhancement of the intensity of tunneling-induced interference, which can be obtained through reducing the dephasing rate of the system. Before starting the following discussion, we would like to introduce an interesting parameter, defined by the ratio $\epsilon_{mn} = \kappa_{mn}/\sqrt{\Gamma_{m0}\Gamma_{n0}}$ ($m,n = 1,2,3$), to assess the strength or quality of the tunneling-induced interference, where the limit values $\epsilon_{mn} = 0$ and $\epsilon_{mn} = 1$ correspond, respectively, to no interference (neglecting coupling between $|m\rangle$ and $|n\rangle$) and perfect interference (no dephasing).

In Fig. 2(a), we plot the evolutions of V_{12}, V_{13}, and V_{23}, when cavity modes a_1 and a_2 are initially in the coherence state $|10, -10\rangle$, and a_3 is in the vacuum state $|0\rangle$. It is clearly shown that V_{12} and V_{13} can be simultaneously lower than 4 during a proper time interval (entanglement period), which demonstrates that the three-mode cavity field will experience the process of product state $\rightarrow$ fully three-mode CV entangled state $\rightarrow$ product state along with the evolution of time. In other words, the fully three-mode CV entangled state can be realized in the present TSQW system. In addition, in Fig. 2(b), we also present the evolution of the total average photon number of cavity modes, $\langle N \rangle = \langle N_1 \rangle + \langle N_2 \rangle + \langle N_3 \rangle$, for the same set of parameters as in Fig. 2(a). The corresponding curve shows that the total average photon number exhibits a fall due to the presence of cavity field losses. It can also be seen that, when the average photon number tends to vanish, correspondingly shown in Fig. 2(a), the entanglement criterion is no longer satisfied since the correlation among the three modes no longer exists.

Next we discuss the influence of tunneling-induced interference strength (assessed by ϵ_{mn}) on the entanglement property. In Fig. 3, we plot the evolutions of V_{12}, V_{13}, V_{23}, and $\langle N \rangle$ when the tunneling-induced interference is enhanced (i.e., ϵ_{21}, from 0.31 to 0.43; ϵ_{31}, from 0.34 to 0.47; ϵ_{32}, from

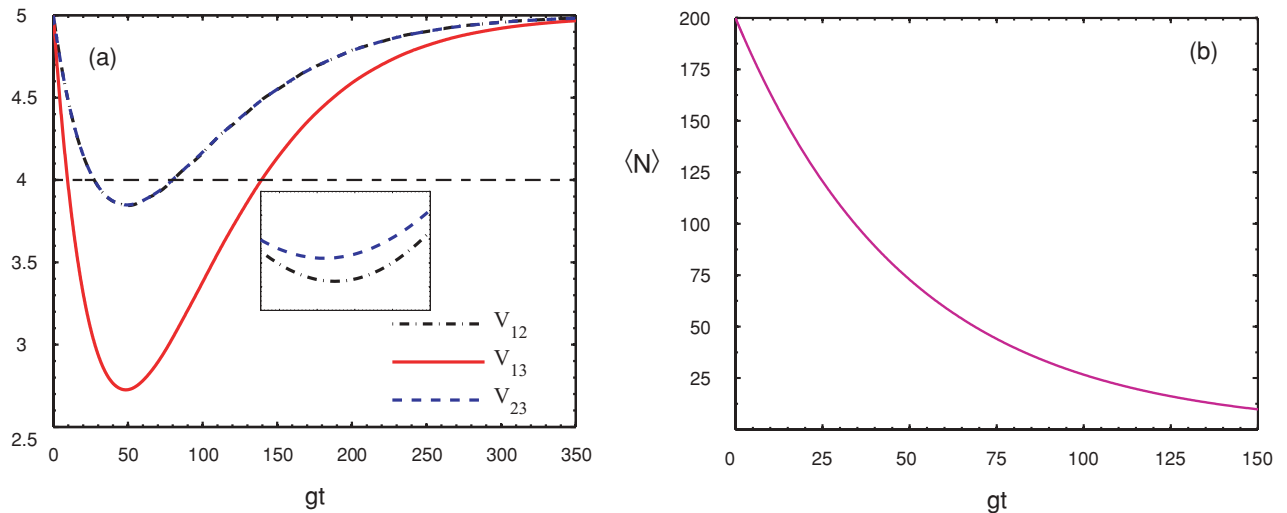

FIG. 2. (Color online) Evolutions of V_{12}, V_{13}, and V_{23} (a) and the average photon number $\langle N \rangle$ (b) in terms of normalized interaction time gt, when the cavity field is initially in the state $|10, -10, 0\rangle$. Various parameters are $\gamma_1 = 1.0$ ps^{-1}, $\gamma_2 = 1.3$ ps^{-1}, $\gamma_3 = 1.7$ ps^{-1}, $\gamma_{10}^{dph} = \gamma_{20}^{dph} = \gamma_{30}^{dph} = 2.5$ ps^{-1} (corresponding to $\epsilon_{21} = 0.31$, $\epsilon_{31} = 0.34$, $\epsilon_{32} = 0.37$), $g_1 = g_2 = g_3 = g = 10^{-3}$ ps^{-1}, and $\kappa_1 = \kappa_2 = \kappa_3 = \kappa = 10^{-5}$ ps^{-1}.
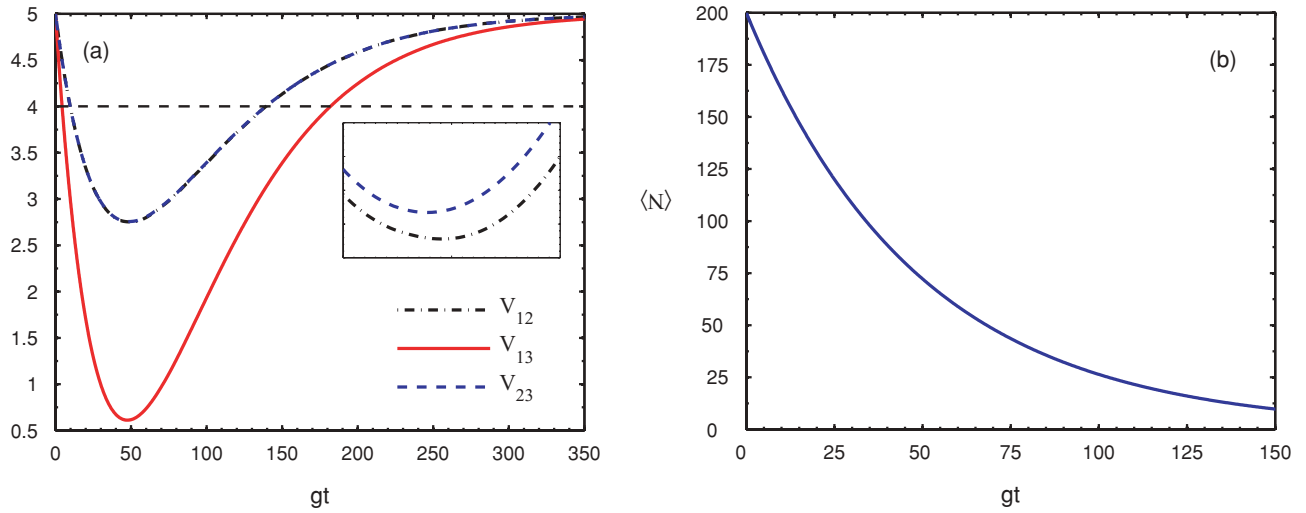
FIG. 3. (Color online) Evolutions of V_{12}, V_{13}, and V_{23} (a) and $\langle N \rangle$ (b) in terms of normalized interaction time gt, when the cavity field is initially in the state $|10, -10, 0\rangle$. Various parameters are the same as in Fig. 2 except for $\gamma_{10}^{dph} = \gamma_{20}^{dph} = \gamma_{30}^{dph} = 1.5$ ps^{-1} (corresponding to $\epsilon_{21} = 0.43$, $\epsilon_{31} = 0.46$, $\epsilon_{32} = 0.49$).

0.37 to 0.49). A comparison of Figs. 2(a) and 3(a) clearly shows that the entanglement period is prolonged effectively due to the increase in the intensity of tunneling-induced interference. This property could be due to the increases in quantum-interference effects among the transitions $|3\rangle \rightarrow |0\rangle$, $|2\rangle \rightarrow |0\rangle$, and $|1\rangle \rightarrow |0\rangle$. Here, it should be pointed out that the increase in the intensity of tunneling-induced interference can be realized through a reduction of the process of higher-interface roughness scattering associated with the dephasing in the TSQW system. To show the influence of tunneling-induced interference on the entanglement period T more distinctly, we also plot the function curves for T versus ϵ_{mn} in Fig. 4. From this figure, we can find that the entanglement period manifests a linearly increasing property with the intensity of

the tunneling-induced interference, which is consistent with our preceding discussion. In addition, it can also be noted from Figs. 2(b) and 3(b) that the influence of tunneling-induced interference on the total average photon number $\langle N \rangle$ is very small. This can be qualitatively explained as follows. In the present scheme, the dominating factor deciding $\langle N \rangle$ is the decay of cavity modes, not the intensity of tunneling-induced interference, which is consistent with Ref. [25].

Up to now, we have demonstrated that the fully three-mode CV entanglement can be realized when the cavity field is initially in the state $|10, -10, 0\rangle$. However, the question that interests us is whether the generation of entanglement is strongly dependent on the initial condition of the cavity field in the present scheme. So, in Fig. 5, we plot the
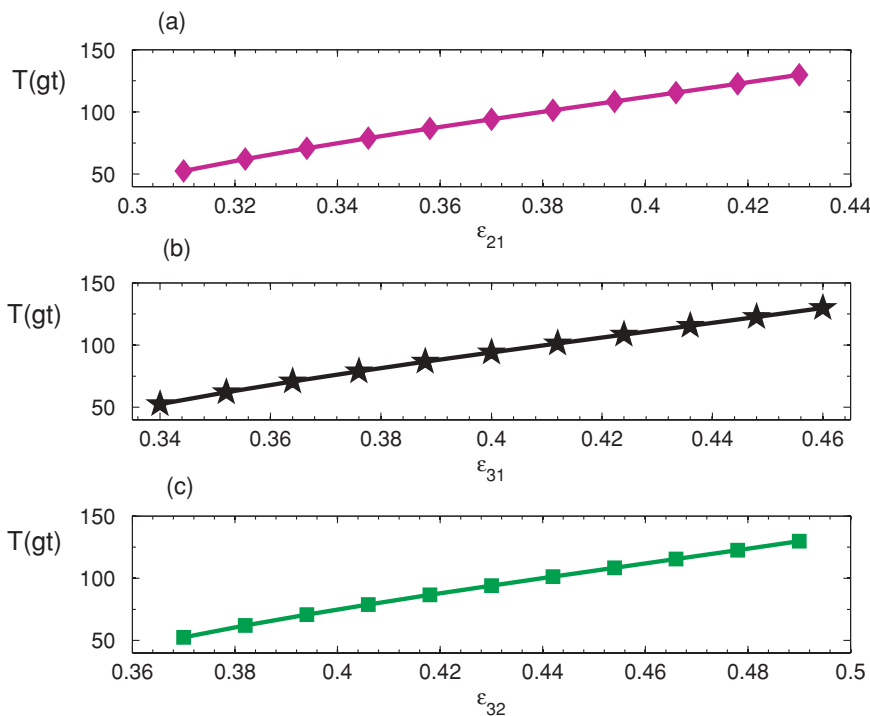

FIG. 4. (Color online) Entanglement period T versus ϵ_{21} (a), ϵ_{31} (b), and ϵ_{32} (c). The other system parameters are the same as in Fig. 2. It should be pointed out that ϵ_{21}, ϵ_{31}, and ϵ_{32} are changed synchronously, and hence (a)–(c) in fact describe the same figure.
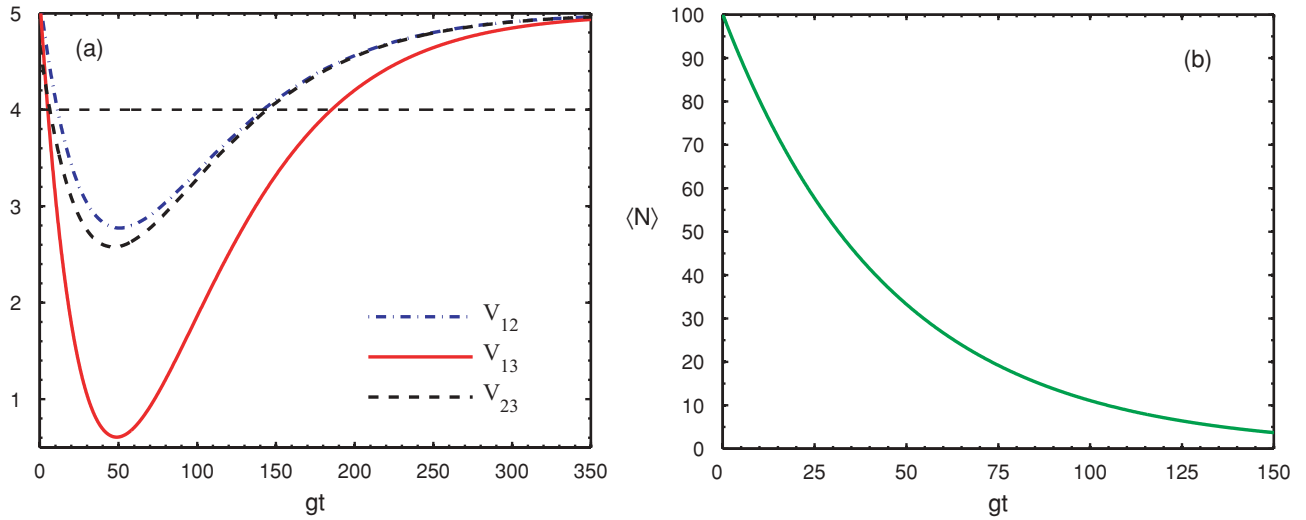
FIG. 5. (Color online) Evolutions of V_{12}, V_{13}, V_{23} (a) and $\langle N \rangle$ (b) in terms of normalized interaction time gt, when cavity mode 1 is initially in the squeezed vacuum state $S(\xi)|0\rangle$, mode 2 is in the coherent state $|\alpha\rangle$, and mode 3 is in the vacuum state. Various parameters are the same as in Fig. 3, except $\xi = 0.2$ and $\alpha = 10$.

evolutions of V_{12}, V_{13}, V_{23}, and $\langle N \rangle$ when cavity mode 1 is initially in the squeezed vacuum state $S(\xi)|0\rangle$, where $[S(\xi) = \exp[(\xi/2)(a_1^2 - a_1^{\dagger 2})]$ and ξ is the squeezing parameter, mode 2 is in the coherent state $|\alpha\rangle$ $(a_2|\alpha\rangle = \alpha|\alpha\rangle)$, and mode 3 is in the vacuum state. It is clearly shown in Fig. 5 that three-mode CV entanglement can still be realized in this situation, which demonstrates the stability of our scheme toward the initial condition. In addition, Fig. 5(b) shows that the average photon number of the cavity field still changes little compared with Figs. 2(b) and 3(b), which further proves that $\langle N \rangle$ mainly depends on the decay of cavity field κ ($\kappa_1 = \kappa_2 = \kappa_3 = \kappa$). In Fig. 6, we present the influence of κ on $\langle N \rangle$ and show that the average photon number $\langle N \rangle$ will fall more rapidly when the decay rate of the cavity field is increased.

Before ending this section, let us briefly discuss the feasibility of our scheme. First, the SQW medium considered

FIG. 6. (Color online) Evolution of $\langle N \rangle$ for different values of cavity field decay rate κ ($\kappa_1 = \kappa_2 = \kappa_3 = \kappa$). Various parameters are the same as in Fig. 3, except $\xi = 0.2$ and $\alpha = 10$.

here can be grown by molecular-beam epitaxy on a GaAs substrate. For more details on this system, we refer the reader to Ref. [50] and references therein. Second, to realize the present scheme, the SQW should have fine quantum-coherence effects, which indeed increases the difficulty of realizing our scheme experimentally. However, the corresponding experimental [46] and theoretical [47,48] studies have demonstrated that the fine quantum-coherence effects can be obtained in the SQW system under proper conditions. In the SQW system, the high dephasing decay rate, determined by electron-electron, interface roughness, and phonon scattering processes, is the major obstacle to obtaining fine quantum-coherent effects. Therefore, it is necessary to tailor elaborately the SQW system considered here (make it with a slick interface and low electron density) to obtain fine quantum-coherence effects and advance the feasibility of our scheme. Finally, in the present scheme, we have assumed that the phonon is strictly confined to an SQW nanostructure and does not influence the surroundings of the SQW nanostructure. It might be difficult to satisfy this ideal condition in practical situations. However, in previous studies on SQWs [46–49], good consistency has been shown between the theoretical outcome under this assumption and the corresponding experimental results. So, the present assumption is valid for an elaborately tailored SQW system. Summing up the preceding discussion, it can be concluded that there indeed are some obstacles for implementation of our scheme experimentally. However, those obstacles can be overcome, in principle, with progress in semiconductor fabricated technology. Therefore, as theoretical research, our scheme is still very significant for stimulating corresponding experiments, such as entanglement in a semiconductor nanostructure.
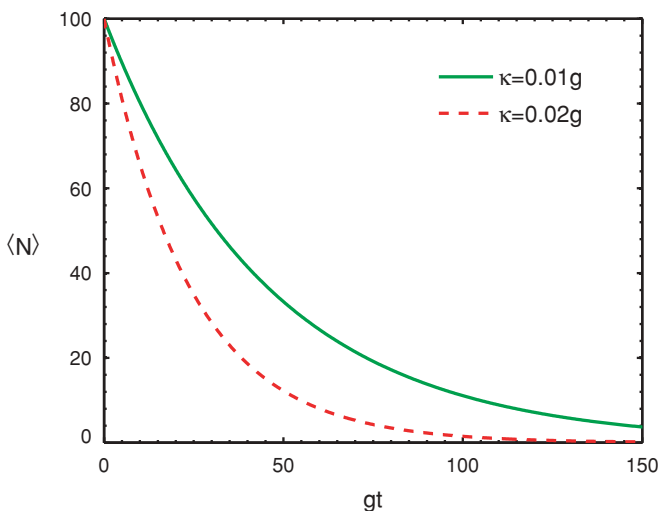
IV. CONCLUSION

In conclusion, based on the standard criteria [26], we have studied the generation of full three-mode CV entanglement

in the TSQW system. The root of entanglement generation here is the quantum coherence between corresponding electron states induced by tunneling in the TSQW system (i.e., tunneling-induced interference effects). By numerically simulating the dynamics of the system, we have studied the influence of tunneling-induced interference on the generation of entanglement and shown that the entanglement period can be prolonged via enhancement of the intensity of this interference. Our research may provide a guideline to achieve three-mode CV entanglement in a semiconductor solid-state system, which is much more practical than its atomic counterpart

because of its flexible design and the controllable interference strength.

[1] M. A. Nielsen and I. L. Chuang, *Quantum Computation and Quantum Information* (Cambridge University Press, Cambridge, UK, 2000).

[2] C. H. Bennett and D. P. DiVincenzo, Nature (London) **404**, 247 (2000).

[3] D. P. DiVincenzo, Science **270**, 255 (1995).

[4] D. Bouwmeester, J. W. Pan, K. Mattle, M. Eibl, H. Weinfurter, and A. Zeilinger, Nature (London) **390**, 575 (1997).

[5] Hiroki Takesue, Opt. Express **14**, 3453 (2006).

[6] X. L. Zhang, K. L. Gao, and M. Feng, Phys. Rev. A **75**, 034308 (2007).

[7] A. K. Ekert, Phys. Rev. Lett. **67**, 661 (1991).

[8] A. Barenco, D. Deutsch, A. Ekert, and R. Jozsa, Phys. Rev. Lett. **74**, 4083 (1995).

[9] Y.-F. Xiao, Z.-F. Han, and G.-C. Guo, Phys. Rev. A **73**, 052324 (2006).

[10] P.-B. Li, Y. Gu, Q.-H. Gong, and G.-C. Guo, Phys. Rev. A **79**, 042339 (2009).

[11] Z. Y. Ou, S. F. Pereira, H. J. Kimble, and K. C. Peng, Phys. Rev. Lett. **68**, 3663 (1992).

[12] J. Fiurasek and N. J. Cerf, Phys. Rev. Lett. **93**, 063601 (2004).

[13] V. Josse, A. Dantan, A. Bramati, M. Pinard, and E. Giacobino, Phys. Rev. Lett. **92**, 123601 (2004).

[14] S. L. Braunstein and P. van Loock, Rev. Mod. Phys. **77**, 513 (2005).

[15] A. Furusawa, J. L. Søensen, S. L. Braunstein, C. A. Fuchs, H. J. Kimble, and E. S. Polzik, Science **282**, 706 (1998).

[16] S. Lloyd and S. L. Braunstein, Phys. Rev. Lett. **82**, 1784 (1999).

[17] L. M. Duan, G. Giedke, J. I. Cirac, and P. Zoller, Phys. Rev. Lett. **84**, 2722 (2000).

[18] R. Simon, Phys. Rev. Lett. **84**, 2726 (2000).

[19] M. Hillery and M. S. Zubairy, Phys. Rev. Lett. **96**, 050503 (2006).

[20] M. Hillery, H. T. Dung, and J. Niset, Phys. Rev. A **80**, 052335 (2009).

[21] H. Xiong, M. O. Scully, and M. S. Zubairy, Phys. Rev. Lett. **94**, 023601 (2005).

[22] L. Zhou, H. Xiong, and M. S. Zubairy, Phys. Rev. A **74**, 022321 (2006).

[23] X.-Y. Lü, J.-B. Liu, L.-G. Si, and X. Yang, J. Phys. B **41**, 035501 (2008); X.-Y. Lü, J.-B. Liu, Y. Tian, P.-J. Song, and Z.-M. Zhan, Europhys. Lett. **82**, 64003 (2008).

[24] M. Kiffner, M. S. Zubairy, J. Evers, and C. H. Keitel, Phys. Rev. A **75**, 033816 (2007).

[25] S. Qamar, F. Ghafoor, M. Hillery, and M. S. Zubairy, Phys. Rev. A **77**, 062308 (2008).

[26] P. van Loock and A. Furusawa, Phys. Rev. A **67**, 052315 (2003).

[27] T. Aoki, N. Takei, H. Yonezawa, K. Wakui, T. Hiraoka, A. Furusawa, and P. Loock, Phys. Rev. Lett. **91**, 080404 (2003).

[28] A. S. Villar, M. Martinelli, C. Fabre, and P. Nussenzveig, Phys. Rev. Lett. **97**, 140504 (2006).

[29] Y. Wu and L. Deng, Opt. Lett. **29**, 1144 (2004).

[30] J. Guo, H. Zou, Z. Zhai, J. Zhang, and J. Gao, Phys. Rev. A **71**, 034305 (2005).

[31] M. K. Olsen and A. S. Bradley, Phys. Rev. A **74**, 063809 (2006).

[32] M. Bondani, A. Allevi, E. Gevinti, A. Agliati, and A. Andreoni, Opt. Express **14**, 9838 (2006).

[33] O. Pfister, S. Feng, G. Jennings, R. Pooser, and D. Xie, Phys. Rev. A **70**, 020302(R) (2004).

[34] A. S. Bradley, M. K. Olsen, O. Pfister, and R. C. Pooser, Phys. Rev. A **72**, 053805 (2005).

[35] Y. B. Yu, Z. D. Xie, X. Q. Yu, H. X. Li, P. Xu, H. M. Yao, and S. N. Zhu, Phys. Rev. A **74**, 042332 (2006).

[36] G.-X. Li, H. Tan, and M. Macovei, Phys. Rev. A **76**, 053827 (2007); G.-X. Li, S. Ke, and Z. Ficek, *ibid.* **79**, 033827 (2009).

[37] X. M. Hu and J. H. Zou, Phys. Rev. A **78**, 045801 (2008); X. Li and X. M. Hu, *ibid.* **80**, 023815 (2009).

[38] X.-Y. Lü, P. Huang, W.-X. Yang, and X. Yang, Phys. Rev. A **80**, 032305 (2009).

[39] J. Faist, F. Capasso, C. Sirtori, K. West, and L. N. Pfeiffer, Nature (London) **390**, 589 (1997).

[40] E. Rosencher and Ph. Bois, Phys. Rev. B **44**, 11315 (1991).

[41] H. Schmidt and A. Imamoğlu, Opt. Commun. **131**, 333 (1996).

[42] J. F. Dynes and E. Paspalakis, Phys. Rev. B **73**, 233305 (2006).

[43] A. Joshi and M. Xiao, Appl. Phys. B **79**, 65 (2004).

[44] A. A. Batista and D. S. Citrin, Phys. Rev. Lett. **92**, 127404 (2004).

[45] J. H. Li, Phys. Rev. B **75**, 155329 (2007).

[46] M. D. Frogley, J. F. Dynes, M. Beck, J. Faist, and C. C. Phillips, Nat. Mater. **5**, 175 (2006); J. F. Dynes, M. D. Frogley, M. Beck, J. Faist, and C. C. Phillips, Phys. Rev. Lett. **94**, 157403 (2005).

[47] J. F. Dynes, M. D. Frogley, J. Rodger, and C. C. Phillips, Phys. Rev. B **72**, 085323 (2005).

[48] G. B. Serapiglia, E. Paspalakis, C. Sirtori, K. L. Vodopyanov, and C. C. Phillips, Phys. Rev. Lett. **84**, 1019 (2000).

[49] M. C. Phillips and H. Wang, Phys. Rev. Lett. **91**, 183602 (2003); Opt. Lett. **28**, 831 (2003).

[50] C. R. Lee, Y. C. Li, F. K. Men, C. H. Pao, Y. C. Tsai, and J. F. Wang, Appl. Phys. Lett. **86**, 201112 (2004).

[51] E. Voutsinas, A. Fountoulakis, A. F. Terzis, J. Boviatsis, S. Baskoutas, and E. Paspalakis, Proc. SPIE **6321**, 63210P (2006).

[52] J. Li, X. Hao, J. Liu, and X. Yang, Phys. Lett. A **372**, 716 (2008).

[53] Y. Wu, L. Wen, and Y. Zhu, Opt. Lett. **28**, 631 (2003).

[54] Y. Wu and X. Yang, Phys. Rev. A **70**, 053818 (2004).

[55] Y. Wu and L. Deng, Phys. Rev. Lett. **93**, 143904 (2004).

[56] Y. Wu, Phys. Rev. A **71**, 053820 (2005).

[57] M. O. Scully and M. S. Zubairy, *Quantum Optics* (Cambridge University Press, Cambridge, 1997), Chap. 14, p. 409.

[58] J. Uffink, Phys. Rev. Lett. **88**, 230406 (2002).

[59] W. Dür, J. I. Cirac, and R. Tarrach, Phys. Rev. Lett. **83**, 3562 (1999).